Inkjet-based technology for microencapsulation of gold nanoparticles within biocompatible hydrogels

Álvaro Artiga, Francisco Ramos-Sánchez, Inés Serrano-Sevilla, Laura De Matteis, Scott G. Mitchell, Carlos Sánchez-Somolinos and Jesús M. de la Fuente**

a. Instituto de Ciencia de Materiales de Aragón (ICMA), Consejo Superior de Investigaciones Científicas (CSIC)-Universidad de Zaragoza and CIBER-BBN, C/Pedro Cerbuna 12, 50009 Zaragoza, Spain
b. Instituto de Nanociencia de Aragón (INA), Universidad de Zaragoza and CIBER-BBN, C/Mariano Esquillor s/n, 50018 Zaragoza, Spain

Á. Artiga, F. Ramos-Sánchez, I. Serrano-Sevilla, Dr. S. G. Mitchell, Dr. C. Sánchez-Somolinos, Prof. J. M. de la Fuente*
Instituto de Ciencia de Materiales de Aragón (ICMA), Consejo Superior de Investigaciones Científicas (CSIC)-Universidad de Zaragoza and CIBER-BBN, C/Pedro Cerbuna 12, 50009 Zaragoza, Spain
E-mail: carloss@unizar.es, jmfuente@unizar.es
Dr. L. De Matteis
Instituto de Nanociencia de Aragón (INA), Universidad de Zaragoza and CIBER-BBN, C/Mariano Esquillor s/n, 50018 Zaragoza, Spain

Keywords: inkjet, gold nanoparticle, encapsulation, chitosan, hydrogel

Herein an inkjet-based technology as a versatile high throughput methodology for the microencapsulation of gold nanoparticles (AuNPs) inside a biocompatible chitosan hydrogel is described. This continuous automated inkjet production approach generates 30 μm diameter polymeric microcapsules and offers high rate of production and nanoparticle encapsulation efficiency of the 14 nm diameter AuNPs, precise control of the microcapsule size and ease of scale-up. The hybrid microcapsules demonstrate biocompatible cell-adhesion properties and resist degradation over a large range of pH, making them particularly relevant for a variety of potential health applications.

Microencapsulation has played centre stage in the biomedical sector for applications such as drug delivery, controlled release and cell/tissue targeting systems.[1] Although frequently employed microencapsulation techniques such as emulsions, extrusion or spray drying[2] are used in industrial production, these methods show several drawbacks including broad size distribution,[3] agglomeration of capsules or low encapsulation efficiency.[4] All of these aspects are of paramount importance in drug delivery systems as the rate of drug release scales with particle size.[5-6] Inkjet-based microsphere production technology offers the potential to improve such limitations to microencapsulation thanks to excellent control and reproducibility of particle size and efficient encapsulation.[7-8] Furthermore, from the industrial perspective, inkjet-based technologies represent continuous microdroplet production systems,[9-10] whereby the process can be fully automated. Importantly, this inkjet set-up can be easily scaled-up using multiple printheads working in parallel with hundreds of inkjet ejection nozzles. Practical aspects such as these can provide advantages for microencapsulation in a number of fields and industries: from the pharmaceutical industry[7-8] to biomedical applications like cell and bacteria microencapsulation.[11-12]

In the biotechnology field, gold nanoparticles (AuNPs) have been used for a number of applications ranging from drug release[13-14] and photothermal therapy[15-16] to biosensing.[17-18] In principle, encapsulating nanoparticles in polymers can be employed to enhance nanoparticle stability, provide sustained release, enhance their bioavailability or improve other aspects related to their delivery and storage.[19] One of the main advantages of encapsulating AuNPs in polymers is that the optical properties of the AuNPs can be preserved,[20] avoiding large unwanted plasmon shifts due to change of solvent and plasmon hybridization.[21] Chitosan is one such naturally occurring biocompatible polymer that has been implemented for oral administration of AuNPs by protecting the nanoparticles in the gastrointestinal tract. Furthermore chitosan is muco-adhesive, which facilitates interaction with the intestinal epithelium enabling their absorption from the intestine into the bloodstream.[22-23]

Here we present an inkjet-based technology for the microencapsulation of gold nanoparticles (AuNPs) within a biocompatible polymeric hydrogel matrix (**Figure 1**). The polysaccharide chitosan (obtained by deacetylation of chitin) was used as the polymeric encapsulating material because of its low cytotoxicity, immunogenicity, muco-adhesive properties and biodegradable characteristics.[24] ~~To the best of our knowledge, this is the first time that inkjet methodology has been employed successfully for microencapsulation using chitosan and also the first time that this technique has been used for encapsulating AuNPs.~~ The benefits of employing this technology include the automatic production of polymeric microcapsules at a high speed and rate of production, combined with high encapsulation efficiency of molecules and nanoparticles in sterile conditions. Sterility is a common and crucial requirement for the use of hybrid materials in biotechnological applications such as oral delivery of anticancer cancer treatments[22] or photothermal therapy.[25]

The inkjet microsphere production setup consists of a piezoelectric printhead equipped with a 50-μm nozzle (see **Figure 1B-C** and **Figure S1**). The piezoelectric element of the microdispenser is controlled using a multichannel device with software that enables the selection of an electrical waveform with defined parameters (rise, fall and pulse frequency, width, times and voltages). In the first instance, the stable and reproducible ejection of chitosan by inkjet was challenging due to tendency of chitosan to form micrometric aggregates that affected the ejection by obstructing the fluidics and clogging the nozzle of the inkjet microdispensing device. In order to avoid these issues, all reagent solutions were passed through a 0.45 μm filter prior to their introduction in the reservoir and a washing protocol using an aqueous acetic acid was used to thoroughly clean the inkjet fluidic system before and after each printing phase (see **Supporting Information**). Different electric waveforms to excite the piezoelectric element were studied, including trapezoidal, bipolar and tripolar, and a comprehensive optimization process was performed controlling all the parameters involved in the excitation pulse including voltage, frequency, duration of the rise and fall of the pulse(s) as

well as pulse width as well as other aspects such as pressure applied to the solution in the fluidic system. By changing the electrical pulse applied to the inkjet nozzle, a continuous ejection of chitosan droplets with a controlled size can be obtained, *e.g.* from 77 µm using trapezoidal down to 51 µm with tripolar (see **Figure S2**), all the while maintaining a stable and reproducible generation of droplets. This decrease in the microdroplet size is a result of the negative pressure induced by the voltage of the tripolar excitation.[26] For the final optimization steps, AuNPs were added to the ejected chitosan solution in order to avoid unwanted changes to the fluid properties that could negatively affect the ejection. Different chitosan concentrations were ejected up to a maximum concentration of 5 mg/mL, above which a stable ejection rate was impeded. This chitosan concentration was established as our reference and the discharge conditions were optimised to achieve a stable and continuous ejection for long periods of time: several hours at a rate of 3000 microdroplets per second at a speed of 2.4 m/s.

Once the inkjet ejection protocol was optimised, different gelling agents to form the microcapsule hydrogels were tested. To facilitate the release of the drugs incorporated in the hydrogel in future applications, negatively charged gelling agents were employed to ionically cross-link the positively charged side chains of the chitosan polymer. To obtain a well-defined microcapsule, an almost instantaneous gelation is needed to maintain the shape of the microdroplets ejected when they enter in the gelling agent solution. A series of different gelling agents at different concentrations described in the literature, including sodium sulphate,[25] tripolyphosphate (TPP),[27] phosphomolybdic acid (PMA)[28] and phosphotungstic acid (PTA),[25] were tested by micropipetting droplets of polymer solution on a receiving solution. When gelling agents such as sodium sulphate and tripolyphosphate were used, they produced slow gelation and as a result heterogeneous amorphous hydrogel fragments were obtained (see **Figure S3**).

Phosphotungstic acid (PTA) has been proven to serve as an efficient gelation agent for chitosan-based materials[28] and has demonstrated its inertness in cell culture.[25] In this inkjet

system the PTA proved to be an instantaneous gelling agent that enabled the formation of the chitosan microcapsules directly upon contact with the gelling solution. It should be noted that microdroplets of chitosan tend to float and form planar aggregates when they were ejected over PTA solution in water. To solve this drawback, the density of gelling agent was decreased by dissolving PTA in an ethanol-water mixture where the optimum gelling conditions were obtained using a 10 mg/mL PTA solution, 60 % (v/v) ethanol solution in water. Another advantage of using ethanol is that it ensures the sterility of microcapsules, as demonstrated by the absence of microorganisms studied by sterility samplers (**Figure S4**). Using this approach and adding the spherical 14 nm diameter AuNPs stabilized with carboxylic acid-terminating polyethylene glycol at a gold:chitosan mass ratio of 0.144 (**Figure S5**) to the chitosan ejection solution, sphere-like homogeneous AuNP-containing chitosan microcapsules were obtained (**Figure 1D**). It should be noted that a controlled agitation of gelling agent was indispensable to avoid aggregation and fusion of microcapsules during the gelation process. These microcapsules were washed with water, concentrated by decantation and their dry weight concentration was measured by freeze-drying (see ESI Materials and Methods). This inkjet set-up and production methodology provided an automatic production rate of 18 mg/hour of microcapsules (**Table 1**) employing just one inkjet microdispensing device with a single nozzle. One of the key advantages of this system is the possibility to scale-up the production employing several multi-nozzle printheads performing a simultaneous ejection in parallel.

Under the conditions reported herewithin, the monodisperse microcapsules with a mean diameter of 34 ± 4 μm were produced (**Figure 2A-B, Figure S10**). Scanning Electron Microscopy (SEM) and Transmission Electron Microscopy (TEM) confirmed that AuNPs were embedded in the chitosan hydrogel matrix (**Figure 2C and S6**). The amount of AuNPs encapsulated in the hydrogel was determined by ICP-AES, and correlated to dry the weight to calculate the AuNPs loading of 2.2 wt.% of gold, which represent an estimated number of 1.3 million AuNPs per microcapsule. The proof-of-concept of our proposed microencapsulation

system provides >90 % encapsulation efficiency (based on the initial concentration of AuNPs ejected) compared to other benchtop chitosan hydrogels containing AuNPs which have shown far lower encapsulation efficiencies near 60%.[25] The high microencapsulation efficiency of this inkjet methodology could be harnessed for encapsulating expensive particles, pharmaceuticals or compounds that are prone to degradation, as is the case for AuNPs. In addition, other molecules of interest can be co-encapsulated along with the AuNPs within in the microcapsules by adding them to the inkjet-ejected solution. We have demonstrated this by the addition of the Alexa 647 fluorophore to the periphery of the microcapsules (**Figure 2D-F**).

The stability of the inkjet microcapsules in physiological and simulated fluids and in different buffers was studied in order to predict the feasibility of using them as potential drug delivery vehicles. The microcapsules possess stability over a wide range of pH displaying almost no liberation of AuNPs from pH 2-9, a moderate 10 % release at pH 10-11 and a complete degradation of the microcapsules with AuNPs releases of greater than 60 % at pH higher than 11 (**Figure 3A**). Crucially, UV-Vis spectra of the AuNPs remained unaltered after their release from the microcapsules (**Figure S7**), indicating that they maintain their colloidal stability without any sign of degradation or aggregation. This post-release colloidal stability is due to the use of –COOH terminated polyethylene glycol as surface stabilising agent for the AuNPs. Here the carboxylic acid PEG improves the stability of AuNPs and enables a better interaction with positively charged chitosan for forming the microcapsules; however, terminal PEG functional groups can of course also be employed for conjugating molecules of interest to the AuNPs.[29] This protective behavior has already been described for other chitosan-AuNPs hybrid systems that protected the functionality of sensitive molecules from gastric degradation.[23] The stability of our inkjet microcapsules was also studied by incubation in simulated gastric fluid that replicates the pH and ion concentration to which microcapsules would be exposed during a potential oral administration route. The release of AuNPs in simulated gastric fluids was studied after 1, 4 and 24 hours of incubation at 37 °C. Overall the

inkjet microcapsules maintained their integrity displaying only minor release of AuNPs (< 10 %) in simulated gastric fluid under all the tested conditions after 24 hours (**Figure 3B**).

As mentioned previously, the cell adhering properties in this type of hydrogel are useful for a wide variety of applications, such as oral delivery[19-22] and nanoparticle-mediated photothermal therapy.[25] Optical microscopy of the interaction between the inkjet microcapsules and cells showed no signs of cellular toxicity or damage (**Figure S8**). The cytotoxicity of the inkjet microcapsules was studied *in vitro* as a preliminary indication of safety for their potential applicability as drug or nanoparticle carriers. MTT cell viability assays showed no cytotoxicity or cell metabolism alteration after 24 hours of incubation of microcapsules with a HeLa cell line at concentrations up to 200 μg/mL (**Figure 3C and S9**).

In conclusion, we have developed an innovative inkjet microencapsulation methodology for trapping nanoparticles within polymeric hydrogels. To the best of our knowledge, this is the first time that inkjet technology has been employed for AuNP encapsulation or for generating chitosan microcapsules. This novel approach enables an automatic production of microcapsules at a high speed and productivity, offering a high production efficiency, degree of control over the size of the microdroplets as well a precise control over the size and shape homogeneity of the corresponding microcapsules. The proof-of-concept 30-μm diameter AuNP-chitosan microcapsules we present show no cytotoxicity and are highly resistant to pH and to degradation in gastric medium. Furthermore, this preparation methodology facilitates the production of sterile microcapsules. This combination of attributes makes the inkjet production methodology highly relevant to a number of biotechnological applications where drug, compound or nanoparticle encapsulation, protection and delivery play key roles for the development of functional materials.

Supporting Information
Supporting Information is available below.

Acknowledgements

Authors thank Spanish MICINN project BIO2017-84246-C2-1-R and DGA and Fondos Feder (Bionanosurf E15_17R). AA acknowledges the Ministerio de Educación, Cultura y Deportes of Spanish Government for an FPU grant (FPU014/06249). ISS acknowledges Ministerio de Economía y Competitividad del Gobierno de España for her FPI grant (BES-2015-071304). The authors also wish to thank The Advanced Microscopy Laboratory (Universidad de Zaragoza) for access to their instrumentation and expertise. They also gratefully acknowledge JC Raposo of the Servicio Central de Análisis de Bizkaia from SGIker of Universidad del País Vasco for ICP-MS or ICP-AES analysis.

References

[1] M. N. Singh, K. S. Y. Hemant, M. Ram and H. G. Shivakumar, *Res. Pharm. Sci.*, **2010**, *5*, 65.

[2] S. Rokka and P. Rantamäki, *Eur. Food Res. Technol.*, **2010**, *231*, 1.

[3] J. Chen, Q. Wang, C. M. Liu and J. Gong, *Crit. Rev. Food Sci. Nutr.*, **2017**, *57*, 1228.

[4] K. Wazarkar, D. Patil, A. Rane, D. Balgude, M. Kathalewar and A. Sabnis, *RSC Adv.*, **2016**, *6*, 106964.

[5] W. J. Duncanson, T. Lin, A. R. Abate, S. Seiffert, R. K. Shah and D. A. Weitz, *Lab Chip*, **2012**, *12*, 2135.

[6] C. Berkland, K. Kim and D. W. Pack, *J. Control. Release*, **2001**, *73*, 59.

[7] S. Hauschild, U. Lipprandt, A. Rumplecker, U. Borchert, A. Rank, R. Schubert and S. Förster, *Small*, **2005**, *1*, 1177.

[8] C. López-Iglesias, A. M. Casielles, A. Altay, R. Bettini, C. Alvarez-Lorenzo and C. A. García-González, *Chem. Eng. J.*, **2019**, *357*, 559.

[9] J. Alamán, R. Alicante, J. I. Peña and C. Sánchez-Somolinos, *Materials (Basel).*, , DOI:10.3390/ma9110910.

[10] B. Derby, *Annu. Rev. Mater. Res.*, **2010**, *40*, 395.

[11] A. K. Anal and H. Singh, *Trends Food Sci. Technol.*, **2007**, *18*, 240.

[12] L. Pedraz, L. U. Wahlberg, P. De Vos and D. Emerich, **2015**, *36*, 537.

[13] Á. Artiga, I. Serrano-Sevilla, L. De Matteis, S. G. Mitchell and J. M. De La Fuente, *J. Mater. Chem. B*, **2019**, *7*, 876.

[14] A. M. Goodman, O. Neumann, K. Nørregaard, L. Henderson, M. R. Choi, S. E. Clare and N. J. Halas, *Proc. Natl. Acad. Sci. U. S. A.*, **2017**, *114*, 12419.

[15] G. Alfranca, Á. Artiga, G. Stepien, M. Moros, S. G. Mitchell and J. M. de la Fuente, *Nanomedicine (Lond.)*, **2016**, *11*, 2903.

[16] A. R. Rastinehad, H. Anastos, E. Wajswol, J. S. Winoker, J. P. Sfakianos, S. K. Doppalapudi, M. R. Carrick, C. J. Knauer, B. Taouli, S. C. Lewis, A. K. Tewari, J. A. Schwartz, S. E. Canfield, A. K. George, J. L. West and N. J. Halas, *PNAS*, **2019**, *116*, 18590.

[17] A. Sguassero, Á. Artiga, C. Morasso, R. R. Jimenez, R. M. Rapún, R. Mancuso, S. Agostini, A. Hernis, A. Abols, A. Linē, A. Gualerzi, S. Picciolini, M. Bedoni, M. Rovaris, F. Gramatica, J. M. de la Fuente and R. Vanna, *Anal. Bioanal. Chem.*, **2019**, *411*, 1873.

[18] H. Yang, Y. Li, D. Wang, Y. Liu, W. Wei, Y. Zhang, S. Liu and P. Li, *Chem. Commun.*, **2019**, *55*, 5994.

[19] N. A. Liechty, W. B., Kryscio, D.R., Slaughter, B. V. and Peppas, *Annu. Rev. Chem. Biomol. Eng.*, **2010**, *1*, 149.

[20] L. M. Liz-marza, M. Giersig and P. Mulvaney, **1996**, *7463*, 4329.

[21] H. Kang, J. W. Lee and Y. Nam, , DOI:10.1021/acsami.7b19342.

[22] S. H. Kang, V. Revuri, S. J. Lee, S. Cho, I. K. Park, K. J. Cho, W. K. Bae and Y. K. Lee, *ACS Nano*, **2017**, *11*, 10417.

[23] G. Barhate, M. Gautam, S. Gairola, S. Jadhav and V. Pokharkar, *Int. J. Pharm.*, **2013**, *441*, 636.

[24] I. Younes and M. Rinaudo, *Mar. Drugs*, **2015**, *13*, 1133.

[25] Á. Artiga, S. García-Embid, L. De Matteis, S. G. Mitchell and J. M. de la Fuente, *Front. Chem.*, **2018**, *6*, 234.

[26] C. Leigh Herran, Y. Huang and W. Chai, *J. Micromechanics Microengineering*, **2012**,

22, 085025.

[27] S. Sreekumar, F. M. Goycoolea, B. M. Moerschbacher and G. R. Rivera-Rodriguez, *Sci. Rep.*, **2018**, *8*, 1.

[28] L. De Matteis, S. G. Mitchell and J. M. de la Fuente, *J. Mater. Chem. B*, **2014**, *2*, 7114.

[29] A. Sguassero, Á. Artiga, C. Morasso, R. R. Jimenez, R. M. Rapún, R. Mancuso, S. Agostini, A. Hernis, A. Abols, A. Lin, A. Gualerzi, S. Picciolini, M. Bedoni, M. Rovaris, F. Gramatica, J. M. De Fuente and R. Vanna, *Anal. Bioanal. Chem.*, **2019**, *411*, 1873.

[30] J. Conde, A. Ambrosone, V. Sanz, Y. Hernandez, V. Marchesano, F. Tian, H. Child, C. C. Berry, M. R. Ibarra, P. V Baptista, C. Tortiglione and J. M. de la Fuente, *ACS Nano*, **2012**, *6*, 8316.

[31] U. Marques, Margareth RC (U.S. Pharmacopeia, 12601 Twinbrook Parkway, Rockville, MD 20852, C. T. 2L7) Loebenger, Raimar (Faculty of Pharmacy and Pharmaceutical Sciences, University of Alberta, Edmonton, Alberta and C. T. 2L7) Almukainzi, May (Faculty of Pharmacy and Pharmaceutical Sciences, University of Alberta, Edmonton, Alberta, *Dissolution Technol.*, **2011**, 15.

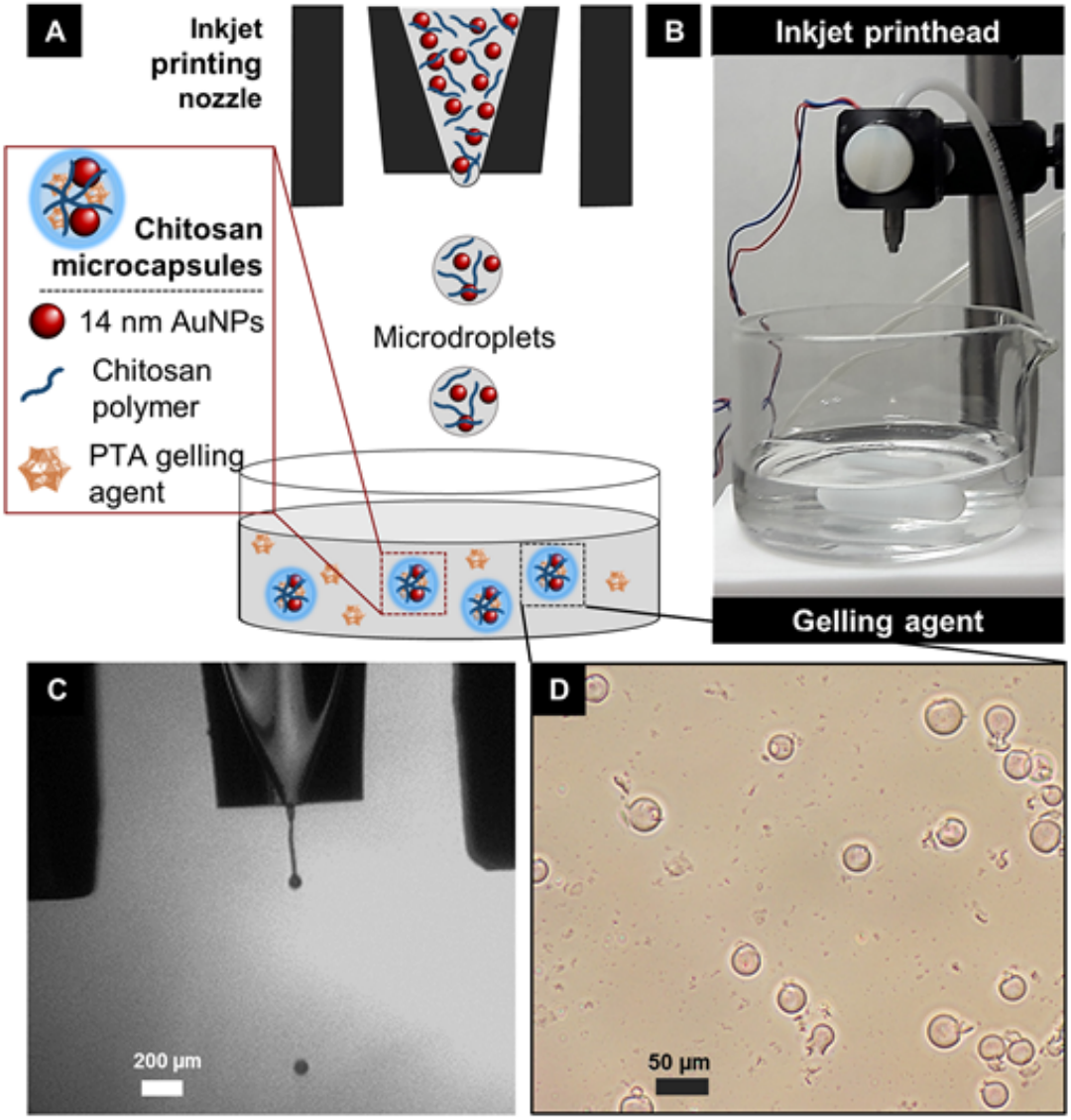

Figure 1. A) Scheme of the inkjet-based methodology employed for AuNP encapsulation in chitosan hydrogel by the production of microdroplets of AuNPs and chitosan solution, using a piezoelectric inkjet printhead. The microcapsules are formed by instantaneous ionic gelation when they enter into contact with the gelling agent phosphotungstic acid (PTA). B) Inkjet system employed for the microdroplet generation. C) Photograph of the chitosan and AuNPs droplets ejected from the inkjet printhead at a rate of 3000 microdroplets per second. D) Optical contrast-phase microscopy image of AuNPs-chitosan microcapsules in water (diameter: 34 ± 4 µm).

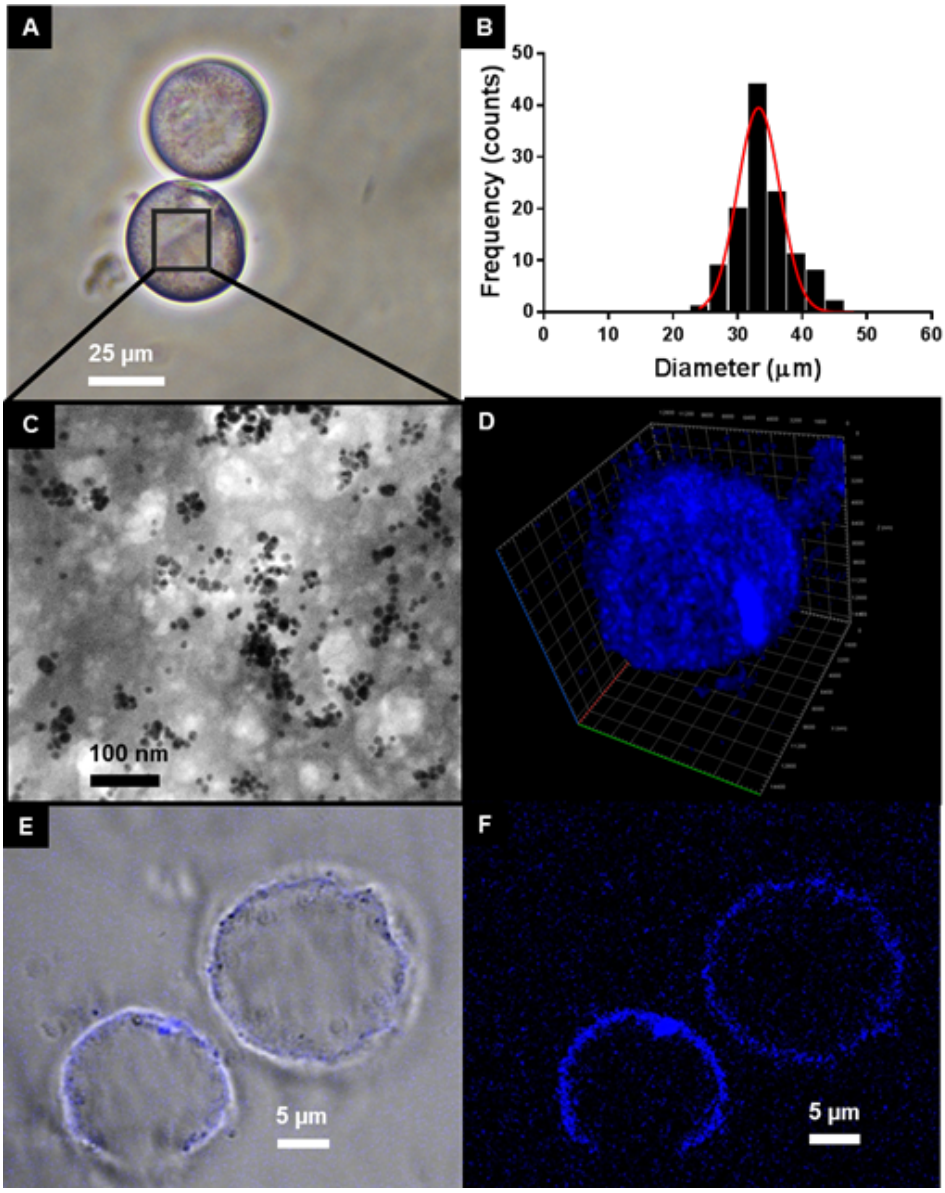

Figure 2. A) Optical contrast-phase microscopy image of chitosan microcapsules containing the AuNPs in aqueous media. B) Size distribution histogram calculated from the measurements taken from brightfield microscopy images. C) Transmission Electron Microscopy image of the hydrogel structure of the microcapsules containing the AuNPs. D) 3D reconstruction of the structure of the microcapsules from the florophore images obtained with the confocal microscopy. E-F) Confocal microscopy image of the microcapsules containing the AuNPs and the fluorophore Alexa 647. The fluorophore is shown in blue in the overlay of the fluorescence and the bright field channels (E) and in the fluorescence cannel (F). It can be appreciated that the Alexa 647 fluorophore is encapsulated in the external part of the microcapsules produced by inkjet.

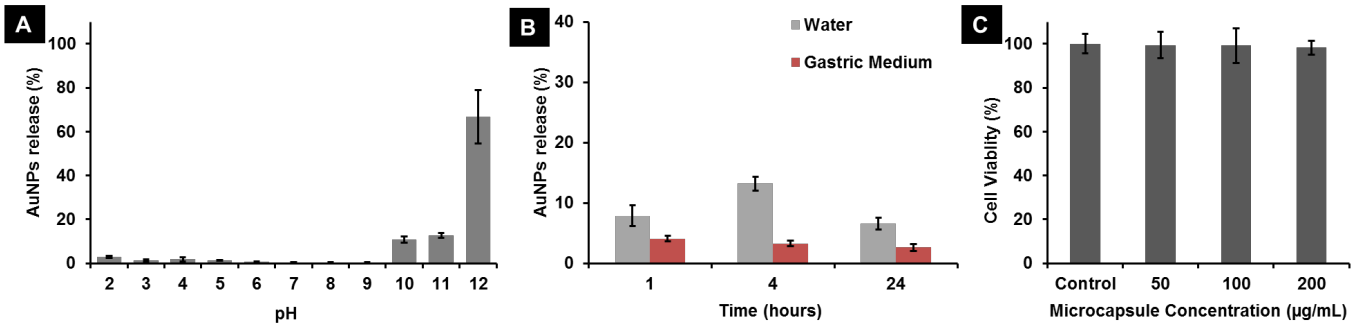

Figure 3. A) pH-dependent release of AuNPs from microcapsules measured after 24 hours of incubation. B) AuNPs release in water and in simulated gastric fluids at different incubation times of 1, 4 and 24 hours. C) HeLa cell viability test by MTT of the microcapsules containing the AuNPs incubated at different concentrations for 24 hours, showing no sign of toxicity.

Table 1. Characteristics of the AuNP microencapsulation in chitosan using inkjet.

Characteristics of AuNP microencapsulation by inkjet	
Encapsulation efficiency (%)	92.4 ± 5.8
Gold loading (% Au/dry weight)	2.2 ± 0.1
Rate of production (mg/h)	18
Frequency (microcapsules/s)	3000
Size (µm)	34 ± 4

Supporting Information

Inkjet-based technology for microencapsulation of gold nanoparticles within biocompatible hydrogels

Álvaro Artiga, Francisco Ramos-Sánchez, Inés Serrano-Sevilla, Laura De Matteis, Scott G. Mitchell, Carlos Sánchez-Somolinos and Jesús M. de la Fuente**

1. Materials and equipment

1.1. Reagents

The reagents used in this study were purchased from Merck KGaA, Darmstadt, Germany, unless otherwise specified. Hydrogen tetrachloroaurate (III) hydrate ($HAuCl_4$) was purchased from Strem Chemicals. Alpha-Thio-omega-(propionic acid) octa(ethylene glycol) (HS- PEG-COOH) (458 g/mol) and was purchased from Iris Biotech GmbH**.** Chitosan of low molecular weight (50-190 KDa) was purchased from Merck Complete Dulbeccos's modified Eagle's medium (DMEM), phosphate buffered saline (PBS) and Dulbecco's Phosphate Buffered Saline (DPBS) supplemented with Ca^{2+} and Mg^{2+} were purchased from Lonza R (Basel, Switzerland). Prior to use, all glassware was washed with *aqua regia* and rinsed thoroughly with Milli-Q water from Millipore Q-POD® system. DMEM was supplemented with 2mM glutamine, 100 U/mL penicillin/streptomycin, and 10 % foetal bovine serum (FBS) for its use in cell culture. For the cell viability assays, MTT (3-(4,5-dimethylthiazol-2-yl)-2,5-diphenyltetrazolium bromide) was purchased from Invitrogen™ (CA, USA). Alexa Fluor 647 alkyne was purchased from Thermofisher Scientific. Coli-Count™ Sampler (Ref. MC0010025), HPC Total Count Sampler (Ref. MHPC10025) and Yeast and Mould Sampler (Ref. MY0010025) were purchased from Merck (Germany).

1.2. Equipment details

UV-Vis-NIR spectra were acquired using a Cary 50 Probe® spectrophotometer from Varian (TO, Italy). For ICP elemental analysis, samples were evaluated by ICP–Atomic emission spectroscopy (AES) using Optima 8300 (Perkin Elmer®, MA, USA). SEM images were collected using a field emission SEM Inspect F50 with an EDX system INCA PentaFETx3 (FEI Company, Eindhoven, The Netherlands) in an energy range between 0-30 keV. TEM images

were collected using a FEI Tecnai TF20 (FEI Europe, Eindhoven, Netherlands) working at 200 kV. Samples were freeze-dried in a Telstar cryodos freeze-dryer (Spain) with an Agilent technologies DS 102 vacuum pump. Confocal microscopy images were acquired employing a Zeiss LSM 880 confocal microscope with an objective 63X, zoom 1.0 and laser source of 633 nm.

1.3. Inkjet set up

The inkjet based microsphere production setup relies on a piezoelectric printhead MJ-ABP-01-50 from Microfab Technologies, Inc with a nozzle of 50 μm. The piezoelectric element of the microdispenser is addressed by using a multichannel JetDrive III device (CT-MC3-4) also from Microfab. Software associated (JetSerer^{TM}, Microfab) enables the selection of an electrical waveform (8 point bipolar trapezoidal waveforms) with well-defined waveform parameters (rise, fall and pulse width, frequency, times and voltages). Pressure and vacuum to control the inkjet dispenser is provided by a CT-PT-4 (Microfab). The software and electronics also controls the strobe LED and the acquisition of the camera to observe the droplet formation process (see **Figure 1** and **Figure S1** for more details). All the solutions were filtered with filters of 0.45 μm (Millex-HV REF SLHV033RS) before been ejected using the inkjet system.

2. Methods

2.1. Gold nanoparticle preparation and characterization

Gold nanospheres (AuNPs) with a diameter of 14 nm and a maximum absorbance peak (LSPR) at 523 nm, were prepared as previously described with minor using the Frens-citrate approach and then coated with HS-PEG-COOH of 458 Da applying the previously reported methodology with minor modifications.[29-30] Briefly, 195 mL of tetrachloroauric acid ($HAuCl_4$) at 1.2 mM was heated until boiling and 5 mL of sodium citrate at 162 mM were added and remained boiling for 30 minutes, light-protected. After that, 10 nM bare gold nanospheres (calculated from ICP-AES quantification) were mixed with 0.028 % sodium dodecyl sulphate, 50 μM HS-PEG-COOH and NaOH 25 mM and incubated for 16 hours in agitation at room temperature. The nanoparticles were washed 3 times by centrifugation for 30 min at 18000 rcf and 4 °C. The pellet of nanoparticles was resuspended in ultrapure water and stored at 4 °C. Extinction coefficient (11.3 $mL \cdot mg^{-1} \cdot cm^{-1}$) was calculated correlating their UV-vis absorbance at 450 nm

with the gold content measured by ICP-AES. The molecular weight of AuNPs was calculated from the diameter of nanoparticles measured from TEM images and the gold density value (19.3 $g \cdot cm^{-3}$).

2.2. Microencapsulation of AuNPs by Inkjet printing

After a carefully optimization of the system parameters, the most consistent ejection was obtained employing the following experimental conditions. 1 mL of chitosan at 10 mg/mL in acetic acid 1 % was mixed with 400 µL of acetic acid 10 % (aq.) and 600 µL of AuNS at 2.4 mg/mL. All the solutions were filtered with filters of 0.45 µm (Millex-HV REF SLHV033RS) before been ejected using the inkjet system. This solution was ejected employing monopolar electric pulse with a rise time of 3 µs, a dwell time of 15 µs and a fall time of 3 µs, a dwell voltage of 32 V and at a frequency of 3000 Hz. The microdroplets ejected with the inkjet over 20 mL of gelling agent solution composed by PTA at 10 mg/mL in 60 % (vol/vol) ethanol (aq.) in mild magnetic stirrer agitation. It was important to carefully wash the inkjet system after the ejection employing 3 volumes of acetic acid 1 % (aq.) in order to avoid future blocking problems due to chitosan residues. After that, the microcapsules were washed 3 times with 10 mL of Milli-Q water by 1 hour of decantation in sterile conditions.

2.3. Characterization of chitosan microcapsules

The concentration of the microcapsules in dry weight was calculated by measuring the weight of 0.2 mL of sample after freeze-drying. The morphology and size of the microcapsules was measured from photographs taken from optical brightfield microscopy images. In order to study the structure and the position of AuNPs inside the hydrogel, the microcapsules were diluted to 0.5 mg/mL in water and 2 µL were deposited on the grid (Ref. CF200-Cu, Electron Microscopy Science), dried at room temperature and analysed in detail by transmission electron microscopy (TEM) and scanning electron microscopy (SEM).

For the co-encapsulation study employing the fluorophore Alexa Fluor 647 Alkyne the microcapsules were produced as previously described just adding Alexa 647 at a final concentration of 10 µg/mL to the ejection solution. The microcapsules produced by this methodology were characterised in solution by confocal microscopy imaging employing a Zeiss LSM 880 confocal microscope with an objective 63X, zoom 1.0 and laser source of 633 nm. The 3D reconstruction was performed using the software Zen Blue 2.3 Lite.

The gold content inside the hydrogel was quantified by inductively coupled plasma atomic emission spectroscopy (ICP-AES). 100 µL of the sample were previously digested by addition of 100 µL of a 3:1 sulfuric acid (96 %)/hydrogen peroxide (33 %) solution and incubated 15 min at room temperature. After that, 300 µL of a 1:3 nitric acid (65 %)/hydrochloric acid (37 %) solution were added. After incubation for 2 h at room temperature the samples were heated to 60 °C for 15 min and they were finally diluted with Milli-Q water up to 20 mL. All samples were prepared and analysed by triplicate. The number of gold nanoparticles per microcapsule was estimated from the frequency of production (3000 microcapsules/s), the reaction production (18 mg/mL) the drug loading (2.2 %) and the molecular weight of AuNP ($1.67*10^7$ g/mol).

The sterility tests were performed according to the supplier instructions, analysing the presence of several microorganisms. The presence of coliform organisms was tested using the Coli-Count™ Sampler, the presence of aerobic bacteria using HPC Total Count Sampler and the presence of yeast or moulds employing the Yeast and Mould Sampler. In detail, the Sampler case was filled with 18 mL of sterile water and 100 µL of sample were added, the Sampler was inserted into the case and maintained in contact with the sample for 30 seconds. After that, the liquid was discarded, the Sampler was reinserted and it was incubated for 48 h at 32 °C for Yeast and Mould, 48 h at 35 °C HPC Total Count and 24 h at 35 °C for Coli-Count™ Sampler.

2.4. AuNPs release from chitosan microcapsules

To study the release of the AuNPs, the microcapsules were incubated with different media. For the pH resistance assay the microcapsules were incubated with sodium phosphate 10 mM at different pHs (2-12). For the oral delivery simulation, simulated gastric medium was employed (NaCl at 34.2 mM at a pH of 1.76).[31] The microcapsules were diluted in the different media until 200 µg/mL in a total volume of 500 µL and were incubated at 37 ℃ with incubation for 1, 4 and 24 hours. After that the microcapsules were centrifuged at 3000 rpm for 5 min in a centrifuge MiniSpin plus and 300 µL were collected for their analysis by UV-Vis spectroscopy and ICP-AES. Experiments were performed in triplicate.

2.5. Biocompatibility of chitosan microcapsules

All *in vitro* studies were performed using HeLa cell line, acquired from Amsbio (Ref. SC034-Puro). Cells were cultured in Dulbecco's modified Eagle's medium (DMEM) supplemented

with 10 % foetal bovine serum (FBS), 2 mM glutamine, and 100 U/mL penicillin/streptomycin at 37 °C, 5 % CO_2 atmosphere.

For the MTT assays, 2.5×10^3 HeLa cells per well were seeded in a 96-multiwell plate and the day after they were incubated with each of the concentrations of the biomaterials for 24 h. At this point, cells were washed 2 times with 200 µL of DPBS and 200 µL of DMEM containing 10 µL of 5 mg/mL MTT were added and they were incubated under culture conditions for 90 min in the dark. Finally, the plate was centrifuged at 1,250 g for 30 min using an Eppendorf centrifuge 5810R with an A-4-62 rotor, the supernatant was removed and the formazan crystals were solubilized with 100 µL of dimethyl sulfoxide (DMSO). After mixing, the optical density at 555 nm was recorded using a plate reader. Experiments were performed in quintuplet and compared with blanks of cells incubated with the microcapsules but without addition of MTT.

3. Supporting Figures

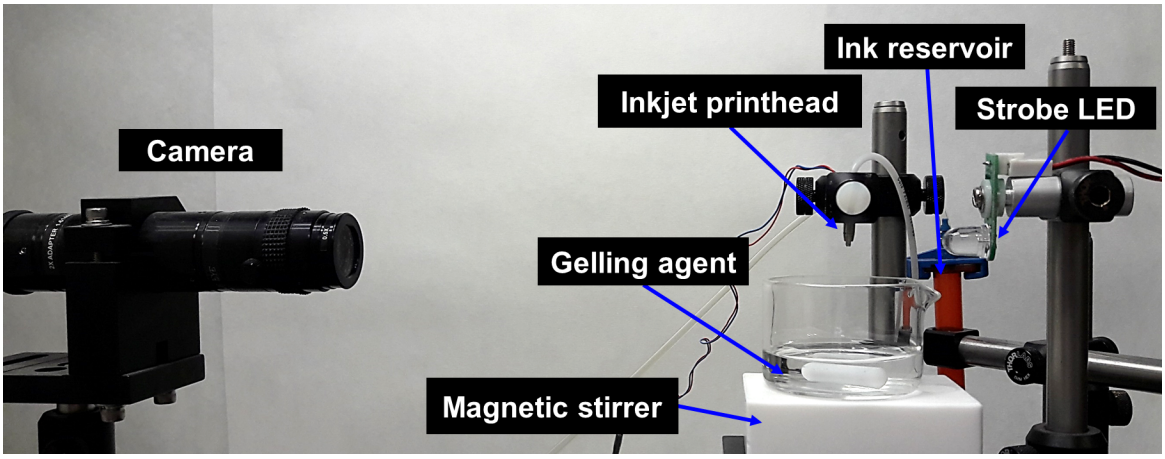

Figure S1. Inkjet system employed for the microdroplet generation, with optical system to monitor the microdroplet ejection.

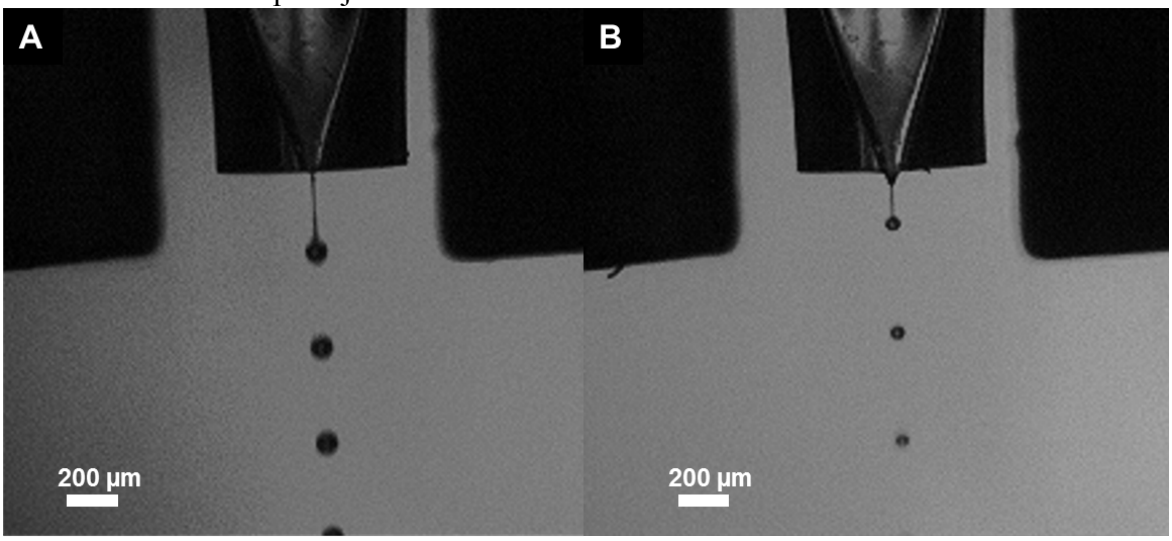

Figure S2. Photographs of inkjet ejection of chitosan 0.1 % (aq.) controlling the size of the microdroplet just by employing different electric pulse waveforms. In this way, it was possible to reduce the size from 77 µm using a trapezoidal waveform to 51 µm using a tripolar waveform.

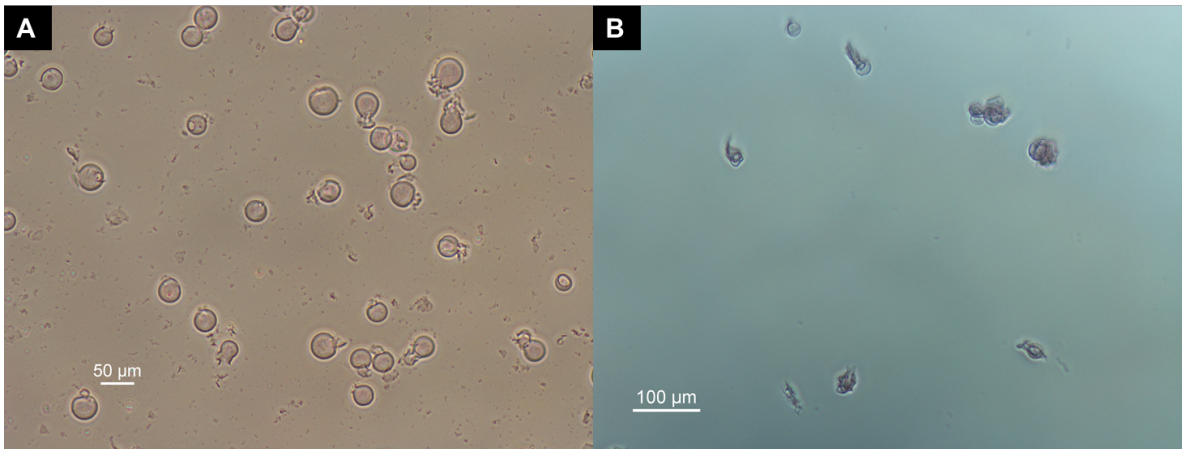

Figure S3. Contrast phase microscopy image of microcapsules synthesised employing PTA (**A**) or tripolyphosphate (**B**) as gelling agent.

Figure S4. Photographs of sterility testers analysing the presence of microorganisms, comparing a negative control (sterile water), two different batches of microcapsules with AuNPs (microcapsules 1 and 2) and a positive control of contamination (ground sample). Coliform organisms were tested using the Coli-Count™ Sampler (blue), aerobic bacteria using HPC Total Count Sampler (red) and yeast or moulds employing the Yeast and Mould Sampler (yellow).

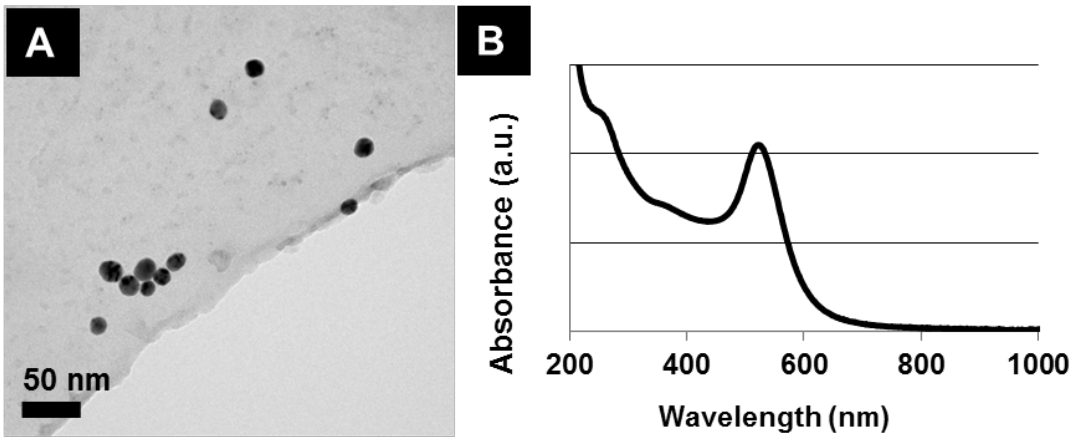

Figure S5. Gold nanoparticle (AuNPs) characterization by TEM (A) and UV-Vis spectroscopy (B) showing the monodispersity, size morphology and localized surface plasmon resonance (LSPR) peak at 522 nm.

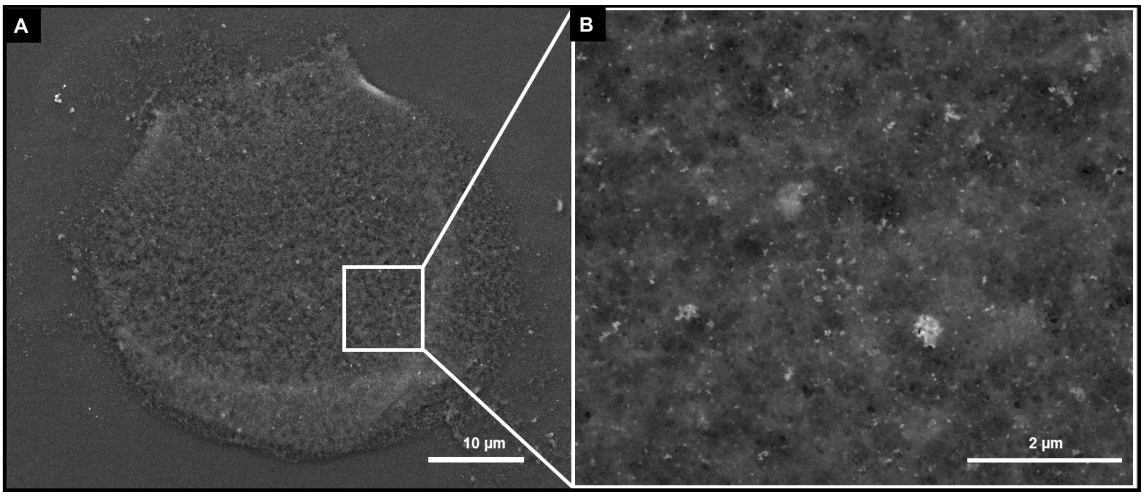

Figure S6. Scanning electron microscopy (SEM) of the microcapsules, showing a complete microcapsule (A) and an amplification (B) showing the AuNPs embedded in the hydrogel structure.

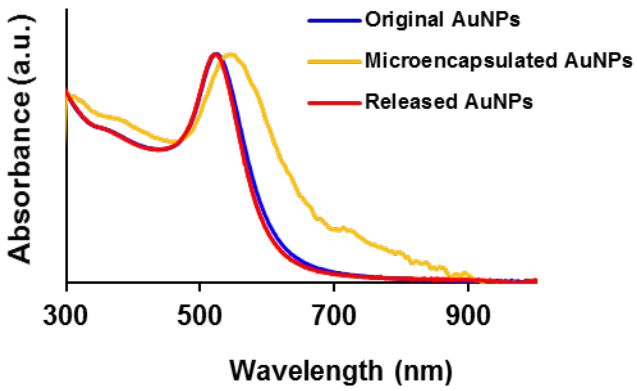

Figure S7. UV-Vis absorbance spectra of AuNPs comparing the AuNPs released from the microcapsules after exposure to pH 12 (Released AuNPs) with the AuNPs before their inkjet microencapsulation (Original AuNPs) along with the AuNPs when encapsulated within the chitosan microcapsules (Microencapsulated AuNPs). It can be seen how the AuNP spectrum after release remains identical to the original AuNPs, indicating the stability of the AuNPs without signs of aggregation or degradation.

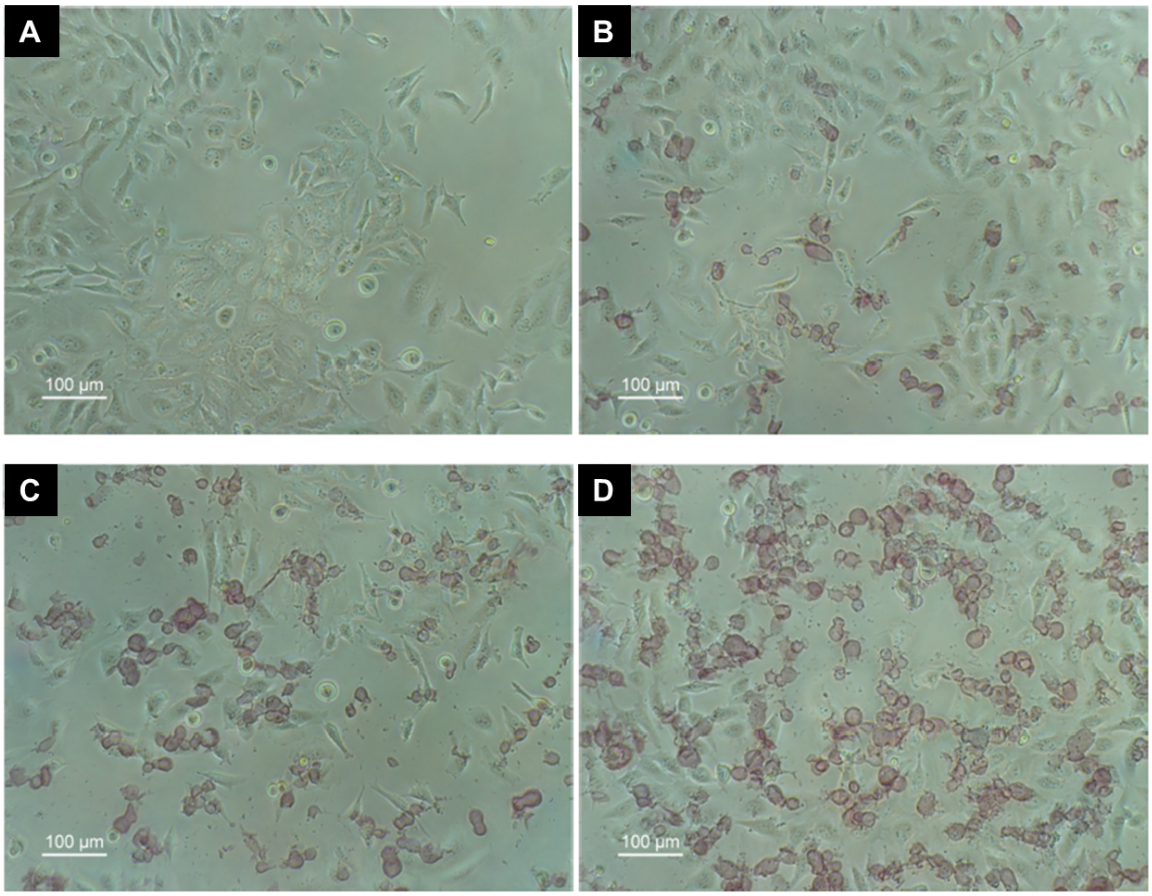

Figure S8. Microscopy images of HeLa cells incubated for 24 hours with 0 (**A**), 50 (**B**), 100 (**C**) and 200 (**D**) µg/mL of microcapsules.

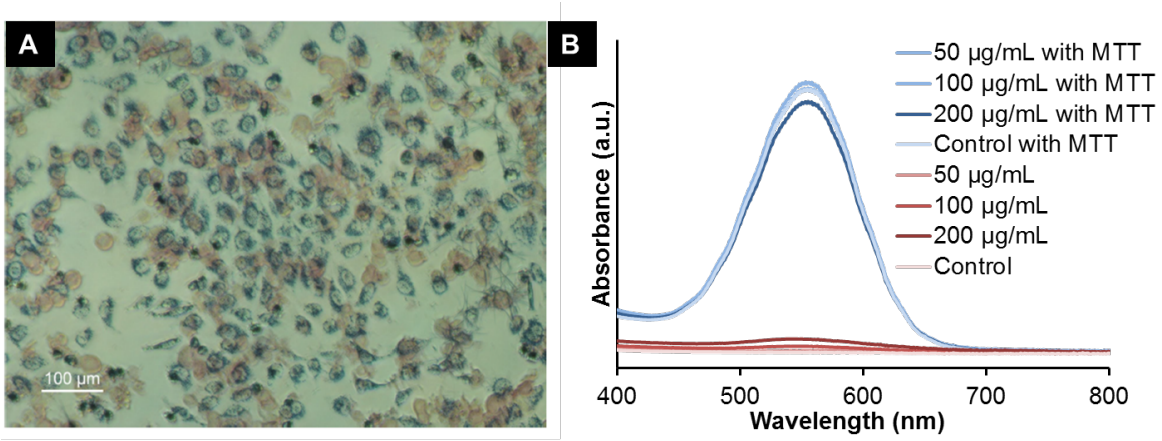

Figure S9. **A**) Microscopy image of HeLa cells incubated for 24 hours with the microcapsules after the MTT assay. **B**) Absorbance UV-Vis spectra of the cells incubated with the microcapsules treated or not treated with MTT, showing a negligible interference of the microcapsules in the MTT assay.

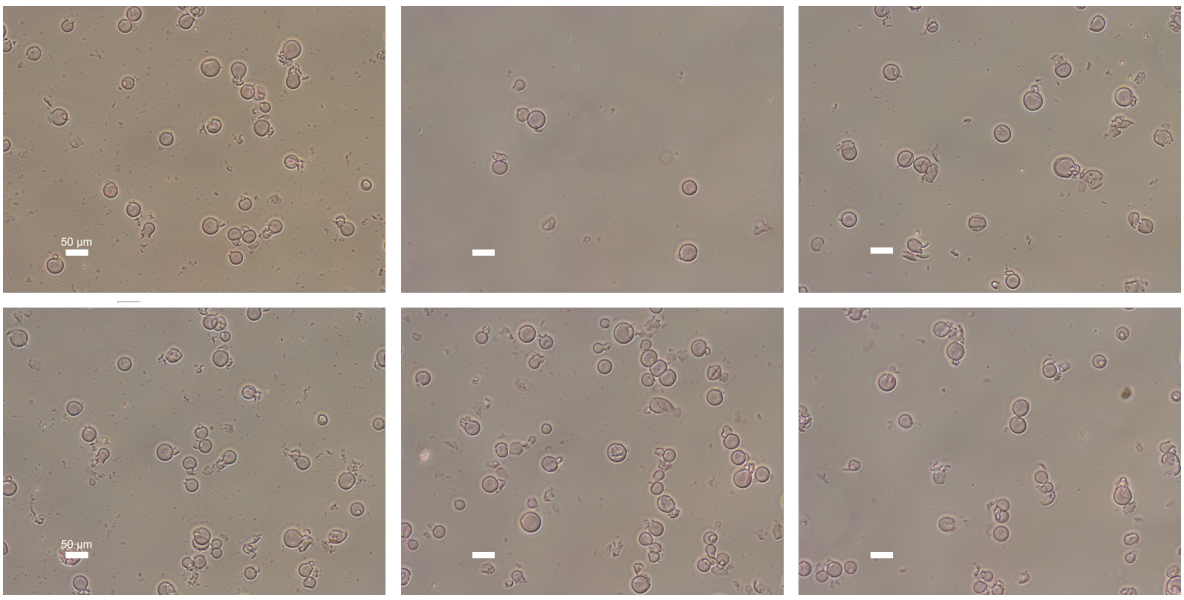

Figure S10. A selection of phase contrast microscopy images of microcapsules employed for histogram distribution in **Figure 2B**. All scale bars correspond to 50 µm.

4. Supporting Bibliography

[1] A. Sguassero, Á. Artiga, C. Morasso, R. R. Jimenez, R. M. Rapún, R. Mancuso, S. Agostini, A. Hernis, A. Abols, A. Lin, A. Gualerzi, S. Picciolini, M. Bedoni, M. Rovaris, F. Gramatica, J. M. De Fuente and R. Vanna, *Anal. Bioanal. Chem.*, **2019**, *411*, 1873.

[2] J. Conde, A. Ambrosone, V. Sanz, Y. Hernandez, V. Marchesano, F. Tian, H. Child, C. C. Berry, M. R. Ibarra, P. V Baptista, C. Tortiglione and J. M. de la Fuente, *ACS Nano*, **2012**, *6*, 8316.

[3] M. R. C. Marques, R. Loebenberg and M. Almukainzi, *Dissolution Technol.,* **2011**, *18*, 15.